Differential effects of diphenyl diselenide $(PhSe)_2$ on mitochondria-related pathways depending on the cellular energy status in Bovine Vascular Endothelial Cells

Letícia Selinger Galant [a,b], Laura Doblado [b], Rafael Radi [c], João Batista Teixeira da Rocha [d], Andreza Fabro de Bem [a,e,f*], Maria Monsalve [b*]

[a] Biochemistry PhD Program, Federal University of Santa Catarina, Florianópolis, SC, Brazil.

[b] Biomedicine Research Institute Sols-Morreale (CSIC-UAM). Arturo Duperier 4. 28029, Madrid, Spain.

[c] Center for Free Radical and Biomedical Research (CEINBIO), Facultad de Medicina, Universidad de la República, Montevideo, Uruguay

[d] Department of Biochemistry and Molecular Biology, Federal University of Santa Maria, Santa Maria, Brazil.

[e] Laboratory of Bioenergetics and Metabolism, Institute for Biological Sciences; University of Brasília, Brasília, Brazil.

[f] National Institute of Science and Technology on Neuroimmunomodulation, Rio de Janeiro, Brazil.

Abstract

Cellular energy metabolism varies depending on tissue and cell type, as well as the availability of energy substrates and energy demands. We recently investigated the variations in cellular metabolism and antioxidant responses in primary bovine vascular endothelial cells (BAECs) under different energetic substrate conditions *in vitro*, specifically glucose or galactose. In this context, pharmacological agents may affect cells differently depending on their energy metabolism status. In this study, we aimed to characterize the effects of diphenyl diselenide ($(PhSe)_2$), a redox-active molecule known for its prominent cardiovascular effects, on redox-bioenergetic cellular pathways under glycolytic or oxidative conditions in BAECs. Under glucose conditions, $(PhSe)_2$ positively impacted mitochondrial oxidative capacity, as assessed by respirometry, and was associated with changes in mitochondrial cellular dynamics. However, these changes were not observed in cells cultured with galactose. Although $(PhSe)_2$ induced the nuclear translocation of the redox sensitive nuclear factor erythroid 2-related factor 2 (Nrf2) in both glucose and galactose media, Nrf2 remained in the nuclei of cells cultured in galactose for a longer duration. Additionally, activation of another redox sensitive transcription factor, forkhead O3 (FOXO3a) was only detected in galactose media. Notably, $(PhSe)_2$ induced the expression of genes controlling mitochondrial antioxidant capacity and glutathione synthesis and recycling in glucose media, whereas its effects in galactose media were primarily focused on glutathione homeostasis. In conclusion, our findings underscore the critical influence of cellular metabolic status on the antioxidant capacity of redox-active molecules such as $(PhSe)_2$.

Key words*:* endothelial cell; diphenyl diselenide, glucose; galactose; mitochondria; FOXO3; Nrf2.

1. Introduction

Cellular energy metabolism may vary depending on the tissue and cell type, the energy substrates available, and the energy demands. Cancer cells, in particular, commonly exhibit a more avid non-oxidative glycolytic metabolism than non-tumor cells [1]. However, they also need to adapt their metabolism in response to substrate availability, which results in corresponding changes in cell physiology and redox-bioenergetic status [2]. Similarly, pharmacology agents may have different cellular effects, depending on the energy metabolism status of the target cells [3].

The use of different cell culture media conditions provides a suitable model for evaluating cellular metabolic performance *in vitro.* While both glucose and galactose are good cellular energy sources, galactose enters the glycolytic pathway through the energy-consuming Leloir pathway [4]. When glucose in the culture medium is replaced by galactose (5-10 mM), cells are forced to shift to the mitochondrial oxidative metabolism to meet their energy demands. This condition not only activates mitochondrial oxidative phosphorylation OXPHOS but fully reprograms mitochondrial function and dynamics and facilitates the evaluation of mitochondrial susceptibility to various agents, revealing sensitivities related to oxidative metabolism that are obscured when cells are cultured in high glucose-containing medium [5,6]. In contrast, glucose catabolism tends to be primarily non-oxidative when glucose levels reach a certain threshold, known as the "Crabtree effect." As a result, cells grown in media with a standard of glucose concentrations (25 mM) tend to acquire a highly non-oxidative glycolytic phenotype [7].

The activation of the mitochondrial OXPHOS is controlled by the master transcriptional coactivator peroxisome proliferator-activated receptor gamma coactivator -1alpha (PGC-1α) and linked to the reprogramming of the cellular capacity to regulate its REDOX status [8]. Furthermore, Nrf2 and FOXO3, transcription factors that control

antioxidant gene expression, and respond to oxidative stress translocating to the nucleus [9,10], are also well known to be sensitive to the cellular metabolic status [11,12], and are regulated by PGC-1α [13,14]. However, studies that evaluate the redox activity of molecules rarely consider the differential effect of the cellular metabolic status. In a recent study, we observed that endothelial cells maintained in a galactose-containing medium, not only exhibited higher mitochondrial oxidative capacity and intercellular metabolic coupling than were cultured in galactose but also showed differences in the nuclear levels of Nrf2 and FOXO3 which may be indicative of differential sensitivity to molecules with redox activity [15], highlighting the relevance of redox-metabolic coupling and the need to control for metabolism in cell assays. Accordingly, it is reasonable to expect that pharmacological drug protocols will have different cellular effects depending on the energy metabolism status of the target cells.

$(PhSe)_2$ is a promising organoselenium compound with antiatherogenic properties [16–18]. The cardiovascular actions of $(PhSe)_2$ have been previously tested in several *in vivo* and *in vitro* models, including hypercholesterolemic mice and rabbits, human low-density lipoprotein (LDL), and vascular endothelial and macrophage cells [19,20]. $(PhSe)_2$, mechanism of action has been proposed to be related to its antioxidant activity. It has been shown to react with reactive cellular redox-sensitive thiols, such as cysteine and the tripeptide glutathione (GSH), an important antioxidant, functioning as a glutathione peroxidase (GPx) mimic, and facilitating the recycling of reduced glutathione. Additionally, $(PhSe)_2$ promotes the oxidation of critical cysteinyl residues in kelch-like ECH-associated protein 1 (Keap1), a redox-sensing protein that retains Nrf2 in the cytoplasm. This oxidation leads to the translocation of Nrf2 into the nucleus and its subsequent activation [16,21–23]. Furthermore, $(PhSe)_2$ has been shown to increase the levels of two key mitochondrial antioxidant enzymes, peroxiredoxin 3 (Prx3) and

101 manganese-dependent superoxide dismutase (MnSOD) [22], which are transcriptional
102 targets of FOXO3 [13] and Nrf2 [24]. However, it must yet be established which
103 transcription factor/s mediate these effects.

104 Therefore, aiming to fully characterize the molecular mechanisms involved in the
105 cardiovascular effects of $(PhSe)_2$ and considering the relevance of metabolic alterations
106 in cardiovascular diseases, we analyzed how $(PhSe)_2$ impacted redox-bioenergetic
107 cellular pathways under glycolytic or oxidative *in vitro* conditions in primary bovine
108 vascular endothelial cells (BAEC).

109 **2. Materials and Methods**

110 *2.1. Cell culture and treatments*

111 BAEC were extracted from a fresh bovine thoracic aorta, obtained in an
112 authorized slaughterhouse, as previously described by Peluffo and colleagues [25]. BAEC
113 were cultured in growth medium (DMEM) supplemented with 10% of fetal bovine serum
114 (FBS; Gibco/Invitrogen), containing 2 mM glutamine, 100 units/mL penicillin, 100
115 μg/mL streptomycin, 10 mM HEPES, 25 mM glucose, 44 mM $NaHCO_3$ and incubated at
116 37°C in a humidified atmosphere with 5% CO_2. Cell suspensions were seeded in 96, 24
117 or 6-well plates (100 × 20 mm), at different cell densities, depending on the experimental
118 procedure. Cells at passages P4–P8 were used to ensure they maintained sufficient
119 mitochondrial plasticity. Cells were allowed to reach 90% confluence and under
120 *glycolytic or oxidative conditions,* as previously described [15], treated with 1 μM $(PhSe)_2$
121 or vehicle (DMSO 0.05%) for 3, 6, 12, 24 or 48h. In short, when BAEC were submitted
122 to the *glycolytic protocol*, culture media was changed to DMEM without FBS and treated
123 with 1 μM $(PhSe)_2$ or vehicle (DMSO 0.05%) for 3, 6, 12, 24 or 48h. When BAEC were
124 submitted to the *oxidative protocol,* culture media was changed to glucose-free RPMI
125 medium with 5 mM galactose and without FBS. Cells were maintained in this medium

126 for 16 hours and then treated with 1 μM $(PhSe)_2$ or vehicle (DMSO 0.05%) for 3, 6, 12,
127 24 or 48h. For each independent experiment, identical cells, derived from the same
128 original culture dish, were split and then exposed to glucose and galactose media
129 separately. Therefore, all the cells within each independent experiment had the same
130 passage. The use of 1 μM $(PhSe)_2$ dosage is based on previous studies from our group
131 and others that demonstrated the protective effect of $(PhSe)_2$ on BAECs at a concentration
132 of 1 μM, as well as the absence of cytotoxic effects [16,17].

133 *2.2. High-resolution respirometry by Seahorse*

134 To evaluate mitochondrial oxygen consumption in BAEC, cells were plated in
135 XF24 cell culture microplates (24-well plates at a cell density of 5 x 10^3 cells/well),
136 submitted to the glycolytic (glucose) or oxidative (galactose) protocols and then treated
137 with 1 μM $(PhSe)_2$ or vehicle for 3, 12 or 48h. A calibration cartridge (Seahorse
138 Bioscience) was equilibrated overnight and then loaded with unbuffered DMEM (port
139 A), 0.6 μM oligomycin (port B), 0.3 μM carbonyl cyanide 4-
140 (trifluoromethoxy)phenylhydrazone (FCCP) (port C), and 0.1 μM rotenone plus 0.1 μM
141 antimycin A (port D), all from Sigma-Aldrich. This allowed the determination of basal
142 respiration, maximal respiration, reserve capacity, and non- mitochondrial respiration. In
143 all experiments, the protein concentration in each well was determined at the end of the
144 measurements, using the Pierce BCA protein assay kit (Thermo Scientific) following cell
145 lysis with RIPA buffer (Sigma-Aldrich) supplemented with a protease inhibitor cocktail
146 (Complete Mini; Roche), and used to calibrate the oxygen consumption data.

147 *2.3. MitoSOX Imaging*

148 Mitochondrial superoxide (O_2^-) was evaluated by MitoSOX Red (Molecular
149 Probes, Carlsbad, CA, USA) staining, essentially as described [26]. Briefly, BAEC were
150 grown on coverslips in 24-well culture (1 x 10^5 cells/well) plates, submitted to the

151 glycolytic (glucose) or oxidative (galactose) protocols and treated with 1 μM $(PhSe)_2$ or
152 vehicle (DMSO 0.05%) for 24h. Then, BAEC were exposed to 500 μM hydrogen
153 peroxide (H_2O_2) for 4h or 80 μM 1,4-naphthoquinone (DMNQ) for 2h, and finally
154 incubated with 3 μM MitoSOX Red for 10 min and fixed with paraformaldehyde (2%)
155 and analyzed by fluorescence microscopy (Nikon 90i). Under our experimental
156 conditions, no nuclear fluorescence was detected, indicating that the probe remained
157 confined to the mitochondria. Therefore, nuclear counterstaining with DAPI or equivalent
158 dyes was not required for image segmentation. For each slide, four images were acquired,
159 and the total fluorescence intensity was determined using ImageJ software. The average
160 fluorescence from the four images was then calculated and considered as the
161 representative fluorescence value for one replica sample.

162 *2.4. Immunofluorescence (IF)*

163 BAEC were grown on coverslips, 24-well culture (1 x 10^5 cells/well) plates and
164 submitted to the glycolytic (glucose) or oxidative (galactose) protocols and then treated
165 with 1 μM $(PhSe)_2$ or vehicle for 3, 6, 12, 24 or 48h. At the end of the incubation period,
166 cells were then fixed with 3.7 % formaldehyde, permeabilized with 0.1 % Triton, and
167 incubated consecutively with a primary antibody Tomm22 (1:200, Sigma Life Science,
168 cat: HPA003037), Nrf2 (1:200, Thermo Fisher, cat: PA5-27882) or FOXO3 (1:100, Cell
169 signaling, cat: 9467) and then a secondary antibody (IgG rabbit ALEXA-488 conjugate,
170 1:2500). Finally, cells were counterstained with DAPI, mounted and examined under a
171 confocal microscope (Zeiss LSM 700, Obercochen, Germany), as previously described
172 [26].

173 Tomm22 was used as a marker to assess mitochondrial content and subcellular
174 distribution using Image J software analysis of confocal microscopy images. Total
175 Tomm22 positive area was considered to indicate mitochondrial volume. Subcellular

176 distribution was analyzed by drawing a ling along the longitudinal cell axis and by
177 calculating the ratio between the perinuclear Tomm22 signal (15 pixels from the nuclear
178 edge) and the total cytosolic signal average provided by that line. Signal asymmetry in
179 the perinuclear region was assessed by calculating the rate of the maximum and minimum
180 intensity values on opposite sides of the nucleus as divided by the above-mentioned cross-
181 section line. Using this line, mitochondrial fission was estimated by the calculation of the
182 standard deviation of Tomm22 signal across the cytosol. The nucleus was identified using
183 the DAPI staining signal, this analysis procedure was as previously described [15,27].
184 Since BAECs are primary cells with significant variability in mitochondrial and
185 respiratory parameters depending on passage number [15], all data were normalized to
186 the t = 0 values of each replica and expressed as a percentage in the graphs.
187 For the analysis of nuclear and cytosolic content of Nrf2 and FOXO3, as previously
188 described [15], a similar procedure was used, using Imagen J Software, a line was drawn
189 across the long axis of each cell the cellular compartment and the nuclear region was
190 identified based on DAPI fluorescence signal. The Nrf2 average fluorescence signal
191 corresponding to the and cytosolic regions was then calculated and then ratio of both,
192 resulting in the nuclear-cytosolic ratio.
193 *2.5. Protein extraction and Western blotting*
194 BAEC (5 x 10^5 cells/well) were grown in 6-well culture plates, submitted to the
195 glycolytic (glucose) or oxidative (galactose) protocols and treated with 1 μM $(PhSe)_2$ or
196 vehicle for 3, 6, 12, 24 or 48h. The cells were then washed with phosphate-buffered saline
197 (PBS) and lysed in 150 μl lysis buffer containing 150 mM NaCl, 0.1% sodium dodecyl
198 sulphate (SDS), 1% sodium deoxycholate, 1% NP40 and 25 mM Tris–HCl pH 7.6, in the
199 presence of protease (Complete, Roche Diagnostics, Mannheim, Germany) and
200 phosphatase inhibitors (Sigma-Aldrich, St. Louis, MO). Cells were harvested by scraping,

201 samples were clarified by centrifugation at 13.000 rpm for 15 min at 4 °C and protein
202 concentration was determined using the BCA assay (Thermo Scientific, Rockford, IL,
203 USA). Equal amounts of protein (40 – 50 µg) from whole extracts were separated by
204 SDS-PAGE electrophoresis, using 10/12% acrylamide/bisacrylamide (29:1) 0.1% SDS
205 gels and transferred to a 0.2 µm PVDF Hybond-P membranes (Amersham/GE healthcare)
206 at 20V for 1h in a semi-dry Trans-Blot SD cell system (Bio-Rad, Hercules, CA).
207 Following the blockade of the membranes using TBS-T (20 mM Tris, 150mM NaCl,
208 0.1% Tween 20) with 3% BSA, they were incubated with primary antibodies and then
209 secondary antibodies in blocking solution, FOXO3 (1:1000, Cell signaling, cat: 9467),
210 pFOXO3 (1:1000, Cell signaling, cat: 2309), Akt (1:1000, Cell signaling, cat: 2920), pAkt
211 (1:1000, Cell signaling, cat: 4060), MnSOD (1:3000, ADI-SOD-110, Enzo Life Sciences,
212 cat: ADI-SOD-110-F), Prx3 (1:1000; LabFrontier, Daehyun-dong Seodaemun-gu Seoul,
213 Korea, cat: LF-PA0030), GCLC (1:1000; Cell Signaling, cat: 48005), GCLM (1:1000;
214 Sigma-Aldrich, cat: SAB5700737) and β-Tubulin (1:80000; Sigma, St. Louis, M, cat:
215 T9026), that was used as loading control. Secondary antibodies rabbit and mouse IgG
216 were from LI-COR Biosciences (Lincoln, NE). Membranes were then extensively washed
217 with TBS-T and developed using Bio-Rad Clarity Western ECL Substrate. Images were
218 captured using a luminometer scanner and subject to densitometry analysis.

219 *2.6. Image analysis*

220 Image J software was used for the analysis of areas, signals in an area and cross
221 section signals from fluorescence and confocal microscopic images for Tomm22, Nrf2,
222 FOXO3 and MitoSOX and to analyze Western blotting membranes.

223 *2.7. Gene expression analysis of genes coding for antioxidant proteins by RT-qPCR*

224 To evaluate mRNA levels, BAEC (5 x 10^5 cells/well) were seeded in 6-well plates
225 and cultivated for 24h. Following cell treatment, total RNA was isolated using TRIzol

226 Reagent (Invitrogen, Carlsbad, CA) following the manufacturer instructions. 1 μg of total
227 RNA was then reverse transcribed by extension of random primers using M-MLV
228 (Promega, Madison,WI). Relative expression levels were determined by real-time PCR
229 (qPCR) in a 7900 Sequence Detection System (Applied Biosystems, Carlsbad, CA) using
230 the primer sets listed below/in Table 1.

231 **Table 1** Primer pairs used in RT-qPCR to quantify gene expression changes.

Target	Forward	Reverse
GCLC	5'-gcacggcatcctccagttcct-3'	5'-tcggatggttggggtttgtcc-3'
GCLM	5'-gtgatgccaccagatttgact-3'	5'-cccactcgtgcgcttgaat-3'
GPx1	5'-ctgctcattgagaacgtagca-3'	5'tctcgccattcacctcgca-3'
MnSOD	5'-ggaacaacaggtcttatccccct-3'	5'-ttacttgctgcaagccgtgtatc-3'
Prx3	5'-ttcgggcttcgctcatccga-3'	5'-atggtatgaggaactggtgct-3'

232

233 *2.8. Statistical analysis and graphics*

234 Numerical raw data was compiled and processed in Excel files (Microsoft) and
235 then final data was incorporated into GraphPad PRISM® software version 6.0 for
236 Windows (GraphPad Software, San Diego, CA, USA), that was used for statistical
237 analysis and preparation of graphs. Normal (Gaussian) distribution was evaluated with
238 the Shapiro-Wilk normality test. Significance of differences among data sets was
239 evaluated using unpaired test *t* or two-way of variance analysis (ANOVA), using
240 Bonferroni's correction for multiple comparisons. Results are expressed as mean ± SD. p
241 <0.05 was considered statistically significant. $n \geq 3$ in all experiments. The number of
242 independent experiments is indicated in the corresponding figure legends. Each data point
243 incorporated in the graphs represents an independent experiment, not technical replicas.
244 Independent means they used an independent vial of cells, thaw on a different day and
245 thus tested on different days. Data from technical replicas/individual cells/individual
246 images were always pooled to calculate each data point. The graphical abstract was

created in BioRender De bem, L. (2025) https://BioRender.com/pu1070I under the agreement number XK28BVWXKS.

3. Results

3.1. Effect of $(PhSe)_2$ on mitochondrial respiration in BAEC

We first tested the differential effect of $(PhSe)_2$ on mitochondrial respiration in BAEC cultured in standard glucose-containing media or in galactose-containing medium to force the cells to rely on OXPHOS for adenosine triphosphate (ATP) production. All control data comparing alterations in BAECs cultured in glucose- versus galactose-containing media have been recently published in [15]. In that study we observed that the maximum oxidative capacity after 12–48 h of incubation of BAEC conditioned in culture medium containing galactose was significantly higher when compared to that observed in cells in culture medium containing glucose. Now, we found that 3h treatment with $(PhSe)_2$ decreased maximum respiration in both glucose- (F (1, 19) = 4,959, p = 0.0382) and galactose- (F (2, 12) = 10,56, p = 0.0023) containing medium (Fig. 1A, C and D) but the oxygen consumption rate (OCR) recovered after 48h of treatment with $(PhSe)_2$ in both glucose- and galactose-containing medium (Fig. 1B, C and D). Furthermore, when the maximum OCR was normalized for the mitochondrial volume, estimated by immunofluorescence analysis of the mitochondrial protein Tomm22, we found that this ratio was significantly increased following 48h of treatment with $(PhSe)_2$ in glucose-containing medium (t = 3.512, p = 0.0246), suggesting a higher respiratory capacity per mitochondria in this context (Fig. 1E). However, in a galactose-containing medium the treatment with $(PhSe)_2$ did not significantly change the maximum respiration/mitochondrial volume unit ratio (Fig. 1F).

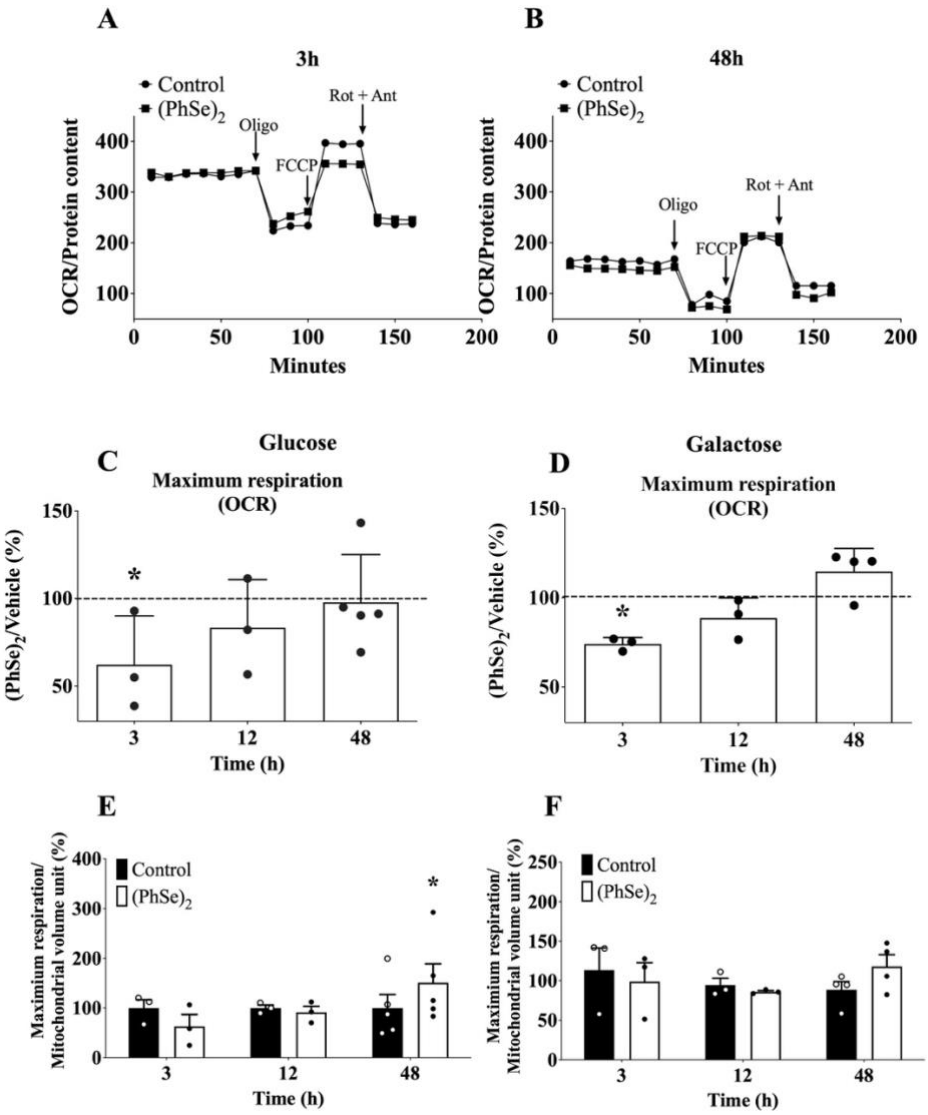

Fig. 1 Effect of $(PhSe)_2$ on mitochondrial respiration in BAEC conditioned in glucose- or galactose-containing medium. (A) Representative respirometry assay of BAEC conditioned in glucose-containing medium for 3h and (B) 48h, data corrected for protein amount. (C) Maximum respiration in BAEC conditioned in glucose-containing medium. (D) Maximum respiration in BAEC conditioned in a galactose-containing medium. (E) Ratio of maximum respiration per mitochondrial volume unit in BAEC treated with $(PhSe)_2$ for 3, 12 or 48h in glucose-containing medium and (F) galactose-containing medium. (A and B) Plots of O_2 consumption (OCR). (C and D) Quantification was corrected using total µg of protein and expressed as the percentage of treatment with $(PhSe)_2$ (white bars) with respect to vehicle group (dashed line). Average points recorded in samples with $(PhSe)_2$ after the addition of FCCP/average points recorded in samples with vehicle after the addition of FCCP x100. (E and F) The mitochondrial volume unit was analyzed by Tomm22 immunofluorescence in 5 independent experiments (Figure 2). The average of the samples after FCCP by Seahorse/average of Tomm22 was analyzed by immunofluorescence. Data were represented as mean ± SD (n=3-5). (C and D) $*p < 0.05$, indicate statistical difference from the vehicle group by two-way ANOVA, followed

288 by Bonferroni's *post hoc* test, (E and F) *$p < 0.05$, indicates statistical difference from
289 vehicle group by paired t-test.
290

291 *3.2. Effect of $(PhSe)_2$ on mitochondrial dynamic in BAEC conditioned in glucose or*
292 *galactose medium*

293 To understand the changes elicited in the mitochondria by $(PhSe)_2$, we monitored
294 mitochondrial dynamics by immunofluorescence analysis of Tomm22 using confocal
295 microscopy. Total mitochondrial volume, fusion, and subcellular distribution were
296 analyzed in BAEC treated with $(PhSe)_2$ for 3, 12, and 48h in glucose- or galactose-
297 containing medium. We found that in glucose-containing medium (Fig 2A-E), although
298 the treatment with $(PhSe)_2$ for 48h decreased total mitochondrial content ($t = 3.161$, $p =$
299 0.0195) (Fig. 2B), it increased mitochondrial fusion ($t = 3.022$, $p = 0.0233$) (Fig. 2C),
300 reduced the mitochondrial content in the perinuclear region ($t = 3.218$, $p = 0.0182$) (Fig.
301 2D), consistent with the observed increase in oxidative capacity per mitochondria.
302 Furthermore, it increased the asymmetrical distribution of mitochondria within the cells,
303 which could be related to intercellular coupling/organization of the epithelium polarity (t
304 $= 3.506$, $p = 0.0172$) (Fig. 2E). In contrast, cells maintained in galactose-containing
305 medium (Fig. 2F-J) did not change the total mitochondrial content (Fig. 2G), fission (Fig.
306 2H), or mitochondrial localization in the perinuclear region (Fig. 2I) in response to the
307 treatment with $(PhSe)_2$. However, a transient increase in the asymmetrical distribution of
308 mitochondria was observed at 12h ($t = 3.041$, $p = 0.0287$), which reverted after 48h ($t =$
309 5.916, $p = 0.001$) of treatment (Fig. 2J).

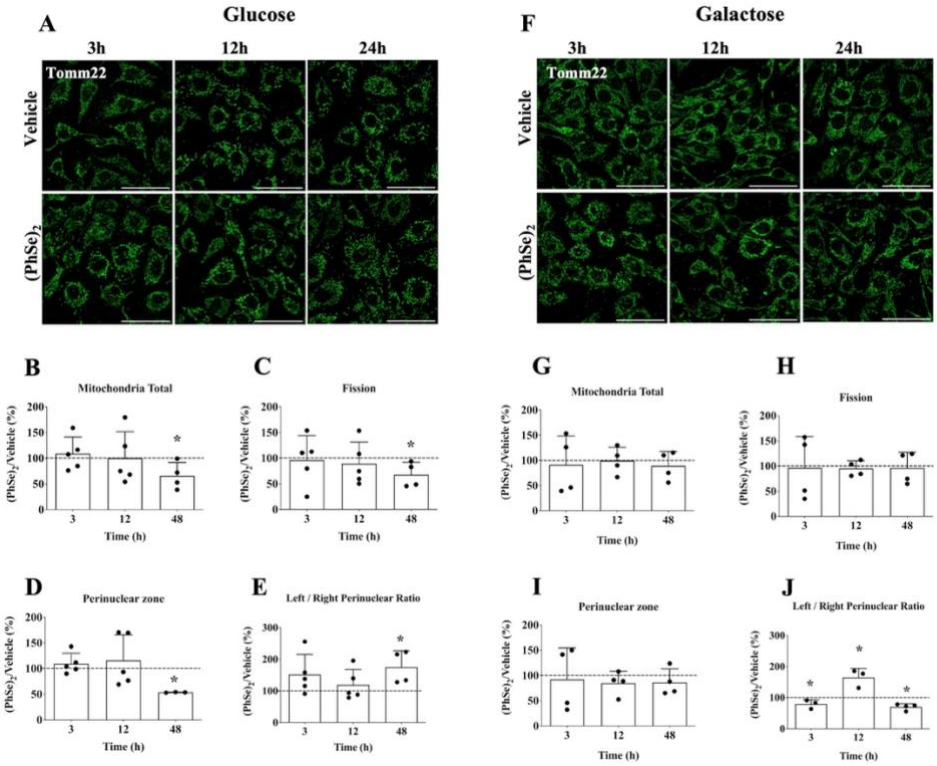

Fig. 2 Effect of $(PhSe)_2$ on mitochondrial dynamics in BAEC conditioned in glucose- or galactose-containing medium. BAEC were treated with $(PhSe)_2$ (1 μM) or vehicle (DMSO) for 3, 12, or 48h in medium containing glucose (A-E) or galactose (F-J), and the mitochondrial parameters were determined by immunofluorescence of Tomm22 antibody. (A and F) Representative image of mitochondrial Tomm22 (green) in BAEC treated with $(PhSe)_2$. The white bars represent 50 μm. (B and G) Quantification of mitochondrial volume, (C and H) mitochondrial fission, (D and I) intensity of the perinuclear zone, (E and J) ratio of left/right intensity. Results were expressed as the percentage of treatment with $(PhSe)_2$ (white bars) with respect to the vehicle group (dashed line). Data were represented as mean ± SD (n=3-4). *$p < 0.05$, indicates statistical difference from vehicle group by unpaired t-test.

3.3. $(PhSe)_2$ prevents the mitochondrial superoxide production in BAEC exposed to oxidants.

To evaluate if $(PhSe)_2$ could modify the cellular capacity to respond to an oxidative challenge, we pre-treated BAEC with 1 μM of $(PhSe)_2$ and then exposed the cells to H_2O_2 (500 μM) or DMNQ (80 μM), an inhibitor of the mitochondrial electron transport chain that drives the formation of mitochondrial superoxide (O_2^-). Mitochondrial RS generation was evaluated using the MitoSOX probe. In BAEC cultured

330 in glucose-containing medium, DMNQ significantly increased O_2^- production.
331 Importantly, $(PhSe)_2$ pre-treatment reduced mitochondrial O_2^- levels in DMNQ
332 challenged cells (F (1,8) = 7.35, p = 0.0266). H_2O_2 in glucose-cultured cells also increased
333 mitochondrial O_2^- levels and, consistently, $(PhSe)_2$ pre-treatment reduced H_2O_2 levels (F
334 (1,7) = 13.66, p = 0.0077) (Fig. 3A-B), suggesting that $(PhSe)_2$ pre-treatment improved
335 mitochondrial homeostasis in glucose cultured BAEC. In contrast, in BAEC cultured in
336 galactose-containing medium, DMNQ did not generate a significant increase in O_2^-
337 production, possibly because in these conditions the mitochondria are more resistant to
338 DMNQ action, while H_2O_2 did. Furthermore, pre-treatment with $(PhSe)_2$ reduced
339 mitochondrial O_2^- levels following H_2O_2 exposure (F (1,7) = 9.171, p = 0.0192) (Fig. 3C-
340 D). These results consistently support the idea that the $(PhSe)_2$ reduces the mitochondrial
341 accumulation of O_2^- levels.

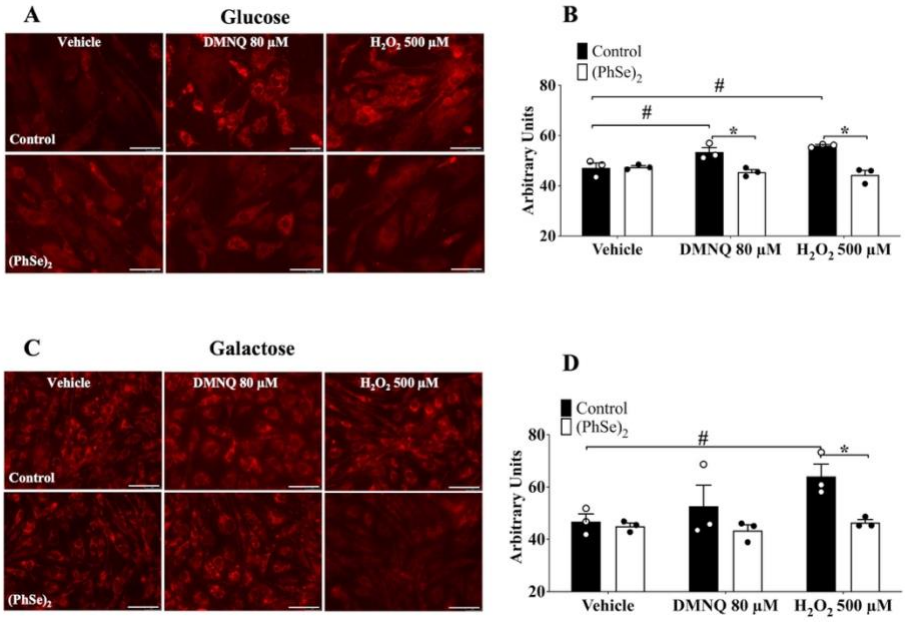

342

343 **Fig. 3** Effect of $(PhSe)_2$ on mitochondrial O_2^- production in BAEC conditioned in glucose-
344 or galactose-containing medium. BAEC were pretreated with $(PhSe)_2$ (1 µM) or vehicle
345 (DMSO) for 24h in medium containing glucose (A-B) or galactose (C-D) and subjected
346 to oxidants as DMNQ or H_2O_2. The O_2^- production was determined by Nikon 90i
347 microscopy through the MitoSOX probe. (A and C) Representative image of
348 mitochondrial O_2^- production in BAEC pretreated with $(PhSe)_2$ and exposed to DMNQ
349 (80 µM) or H_2O_2 (500 µM) (for 2 or 4h, respectively), the white bars represent 50 µm. (B

350 and D) Quantification of mitochondrial O_2^- production (values x 10^4) in BAEC pretreated
351 with $(PhSe)_2$ and exposed to DMNQ or H_2O_2. * $p < 0.05$, indicates statistical difference
352 between the groups exposed to oxidants and $(PhSe)_2$, # $p < 0.05$, indicates the statistical
353 difference between vehicle and DMNQ or H_2O_2 groups by two-way ANOVA, followed
354 by Bonferroni's *post hoc* test.
355

356 *3.4. Time-course effect of $(PhSe)_2$ in the expression of antioxidant proteins in BAEC*
357 *conditioned in glucose or galactose medium.*

358 Next, we decided to evaluate if the observed effect of $(PhSe)_2$ on mitochondrial
359 O_2^- levels could be derived from an increased cellular detoxification capacity. To that
360 end, we used targeted gene expression and protein analysis of some major antioxidant
361 coding genes regulated by the two crucial redox-sensitive transcription factors, Nrf2 and
362 FOXO3. In BAEC cultured in glucose-containing medium, following 6h of treatment
363 with $(PhSe)_2$ we observed a significant increase in MnSOD and *SOD2* gene expression
364 levels (F (3,47) = 5.159, p = 0.0036 and F (1,29) = 7.157, p = 0.0121, respectively) (Fig.
365 4A-B) as well as an increase in Prx3 protein levels (F (3,36) = 2.722, p = 0.053) (Fig. 4C-
366 D). Both MnSOD and Prx3 are antioxidant proteins that localize in the mitochondrial
367 matrix. We also monitored the effect of $(PhSe)_2$ on GCL, the enzyme of the limiting step
368 for the synthesis of the antioxidant tripeptide glutathione, and GPx1, the main enzyme
369 involved in the recovery of reduced glutathione following its oxidation, in glucose-
370 containing medium. GCL is made up of two subunits. We noted that GCLC protein and
371 *GCLC* gene expression levels increased (F (1,20) = 30.42, p<0.0001 and F (1,27) = 16.94,
372 p = 0.0003, respectively) following 24h of treatment with $(PhSe)_2$ (Fig. 4E-F) as well as
373 *GCLM* levels at 6h of treatment (F (1,30) = 8.759, p = 0.006) (Fig. 4 G-H). Furthermore,
374 *GPx1* levels were increased at 12 and 24h of treatment with $(PhSe)_2$ in BAEC cultured in
375 glucose-containing medium (F (1,14) = 29.11, p < 0.0001) (Supplementary Fig. 1A).
376 Similar results were observed in BAEC maintained in a galactose-containing medium.

377 We observed an increase in the mRNA levels of *GCLC* after 12h (F (1,22) = 14.07, p =
378 0.0011) and GCLC protein content at 24h (F (1,31) = 9.316, p = 0.0046) (Fig. 4 M-N), as
379 well as an increase in GCLM protein levels after 6h of treatment with $(PhSe)_2$ (F (3,14)
380 = 5.9, p = 0.0076) (Fig. 4 O-P). $(PhSe)_2$ also increases the mRNA expression of GPx1 at
381 12 and 24h of treatment in the galactose-containing medium (F (1,12) = 40.22, p <
382 0.0001) (Supplementary Fig. 1B). In contrast, *SOD2* mRNA levels and protein of
383 MnSOD were unaltered (Fig. 4 I-J), while the Prx3 levels decreased after 24h of treatment
384 with $(PhSe)_2$ in the galactose-containing medium (Fig. 4 K-L). The mRNA levels of
385 catalase (*CAT*), mitochondrial uncoupling protein 2 (*UCP2*), cytochrome c (*CYTC*),
386 glutathione synthetase (*GSS)* and *Nrf2* were unaltered by the treatment with $(PhSe)_2$ of
387 BAEC maintained in either glucose- or galactose-containing medium (Supplementary
388 Fig. 1 C-L). Overall, these results suggest that in glucose containing media $(PhSe)_2$
389 induces both the main mitochondrial and cytosolic antioxidant systems, while in galactose
390 media $(PhSe)_2$ induces mainly the cytosolic antioxidant systems, a result consistent with
391 the expected pre-activation of OXPHOS and mitochondrial antioxidant capacity in
392 galactose media.

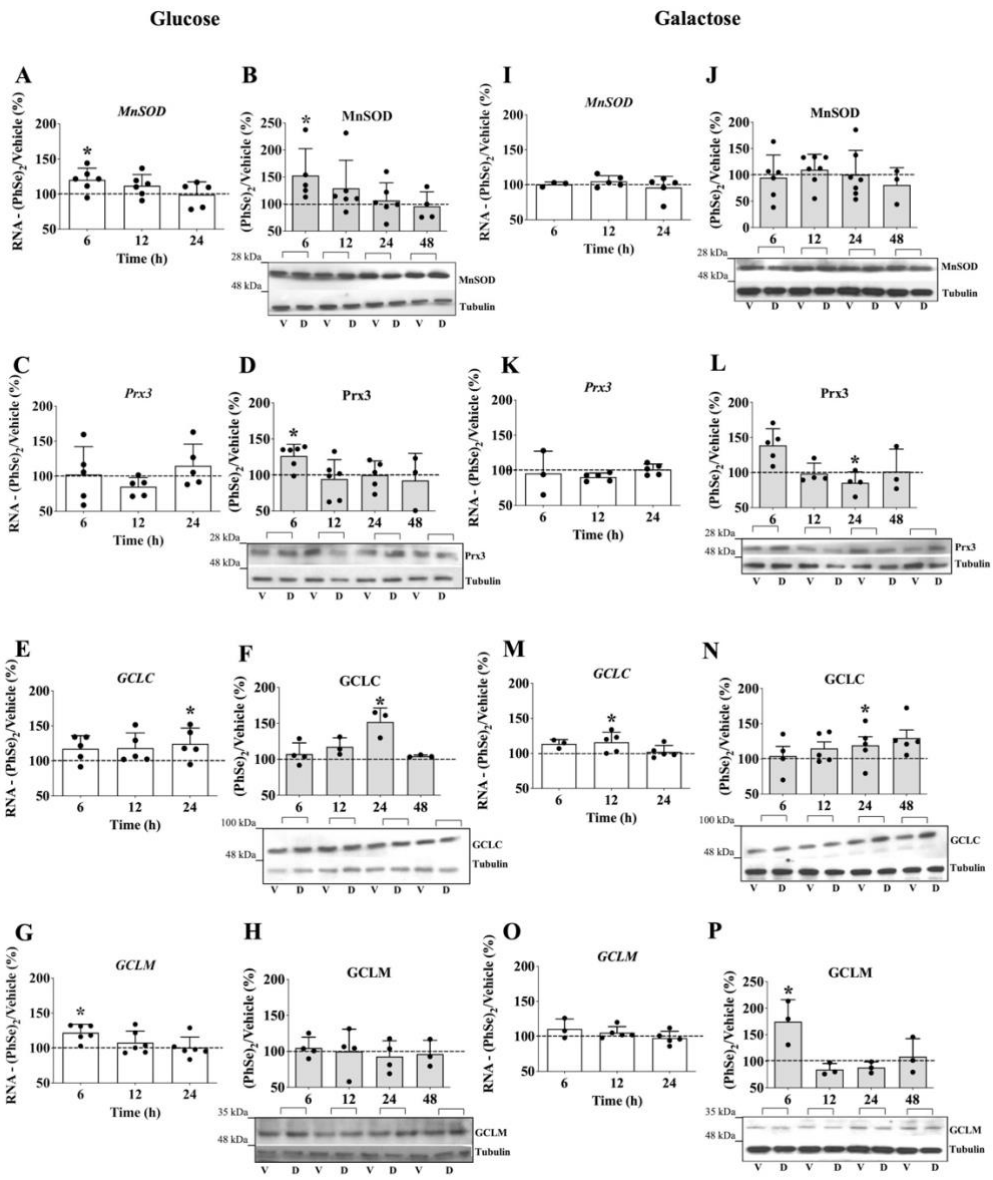

Fig. 4 Effect of $(PhSe)_2$ in time-course expression profiles of antioxidant proteins in glucose- or galactose-containing medium. BAEC were treated with $(PhSe)_2$ or vehicle (DMSO) for 6, 12, 24 or 48h in glucose or galactose medium. Protein expression by Western Blotting analyses and mRNA expression by qPCR. Results were expressed as protein /β-tubulin ratio and the data were presented as the percentage of treatment with $(PhSe)_2$ (bars) with respect to vehicle group (dashed line). V = vehicle, D = $(PhSe)_2$. Data were represented as mean ± SD (n=3-7). *$p < 0.05$, indicate statistical difference from vehicle group by two-way ANOVA, followed by Bonferroni's *post hoc* test.

3.5. Effect of $(PhSe)_2$ on Nrf2 nuclear translocation of BAEC conditioned in glucose or galactose medium.

405 Since $(PhSe)_2$ increased the levels of antioxidant genes known to be targeted by
406 the transcription factor Nfr2, we evaluated the effect of $(PhSe)_2$ on Nrf2 nuclear
407 translocation, a thus activation, in BAEC cultured in glucose- or galactose-containing
408 medium. We found that Nrf2 nuclear localization was increased following 3h of
409 incubation with $(PhSe)_2$ in BAEC cultured in both glucose and galactose containing
410 medium (F (4,14) = 4.737, p = 0.0126 and F (1,30) = 64.98, $p < 0.0001$, respectively)
411 (Fig. 5A-B). The increased nuclear localization was gradually reduced overtime in both
412 glucose and galactose cultured cells but was maintained over a more extended period in
413 galactose cultured cells (Fig. 5C-D), suggesting a more effective nuclear retention in
414 galactose. The separate evaluation of nuclear and cytosolic levels of Nrf2 showed a
415 significant increase in cytosolic Nrf2 levels following 3h of treatment with $(PhSe)_2$ in
416 BAEC maintained in glucose- containing medium but not in galactose cultured cells
417 possibly suggesting that global Nrf2 levels stabilized by $(PhSe)_2$ in glucose but not in
418 galactose media (Supplementary Fig. 2). Nrf2 degradation is a tightly regulated process,
419 cytosolic retention of Nrf2 by Keap1 is linked to its proteasomal degradation, and
420 therefore, Keap1 release is generally associated not only to Nrf2 nuclear translocation but
421 also to its stabilization [28]. In summary, Nrf2 activation is detectable in both glucose
422 and galactose media, but in galactose media is likely to be effective for more extended
423 periods of time.

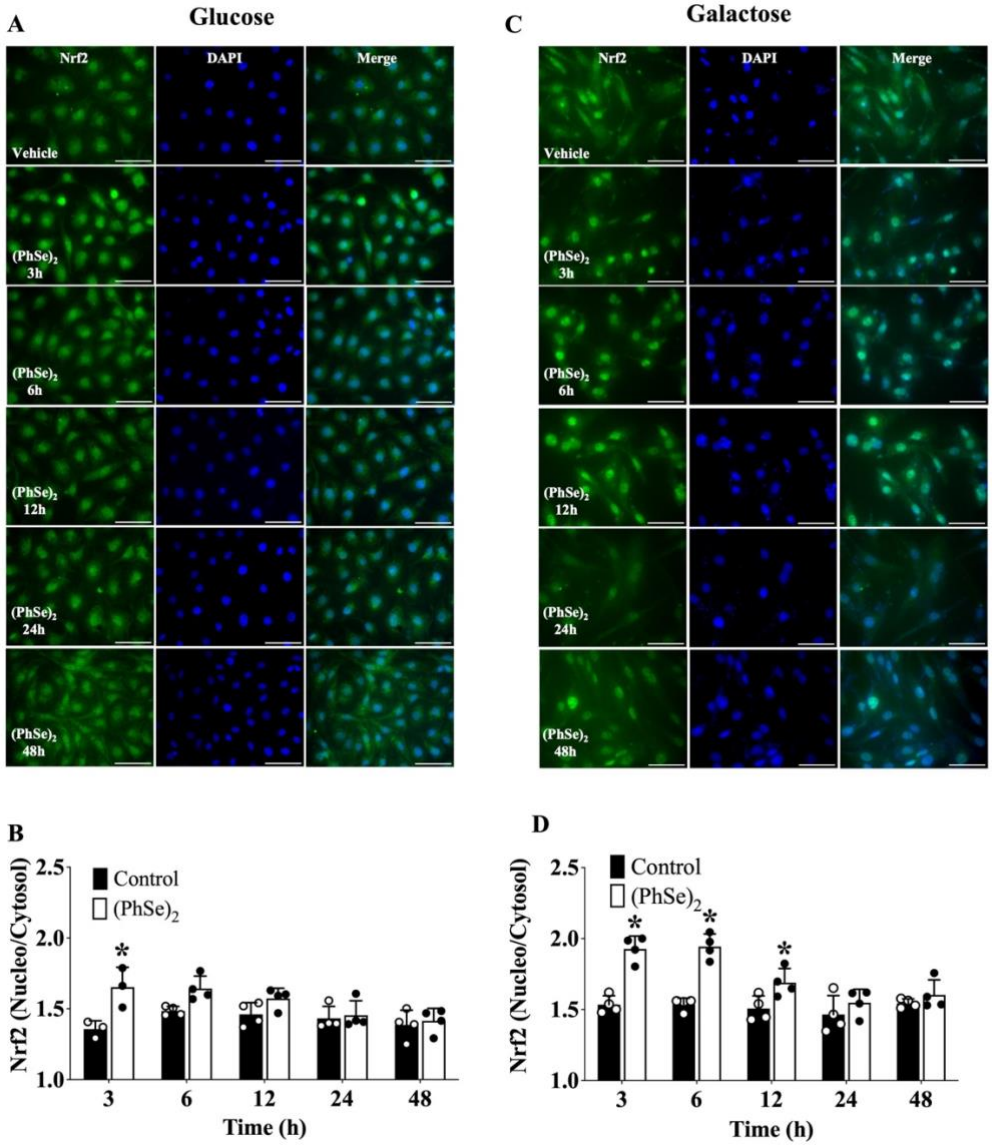

Fig. 5 Effect of $(PhSe)_2$ on Nrf2 translocation in BAEC conditioned in glucose- or galactose-containing medium. BAEC were treated with $(PhSe)_2$ (1 µM) or vehicle (DMSO) for 3, 6, 12, 24 and 48h in medium containing glucose (A-B) or galactose (C-D) and the immunofluorescence the Nrf2 were analyzed. (A and C) Representative image of immunofluorescence from Nrf2 (green) and DAPI (blue) in BAEC, the white bars represent 50 µm. (B and D) Ratio of Nrf2 in the nuclei/cytosol. Data were represented as mean ± SD (n=3-4). * $p < 0.05$, indicate statistical difference from vehicle group by two-way ANOVA, followed by Bonferroni's *post hoc* test.

3.6. Effect of $(PhSe)_2$ on FOXO3 activation in BAEC conditioned in glucose or galactose medium.

436 Finally, we also analyzed the possible involvement of FOXO3 transcriptional
437 factor in $(PhSe)_2$ activation of antioxidant gene expression. Treatment of BAEC in
438 glucose-containing medium with $(PhSe)_2$ for 6, 12 or 24h increased the level of FOXO3
439 phosphorylation (pFOXO3) at Thr32 (F (1,90) = 8.111, p = 0.0055), a mark of Akt
440 phosphorylation (pAkt), suggesting an inhibition of FOXO3 activity and nuclear
441 extrusion (Fig. 6A). However, no significant changes in the nuclear/cytosolic ratio of
442 FOXO3 (Fig 6E) nor in the cytosolic and nuclear levels when analyzed separately
443 (Supplementary Figure 3), and, although an increase in Akt phosphorylation was
444 detectable in response to $(PhSe)_2$, it could only be observed at 24h of treatment in glucose
445 media (F (1,76) = 12.86, p = 0.0006) (Fig. 6C). In contrast, although the nuclear/cytosolic
446 ratio of FOXO3 transiently decreased at 3h of treatment in galactose media (Fig. 6F),
447 $(PhSe)_2$ decreased pFOXO3/FOXO3 ratio at 24h (F (3,57) = 5.642, p = 0.0019),
448 suggesting an increase in FOXO3 activity and nuclear localization (Fig. 6B). In these
449 conditions although the changes in pAkt levels did not reach statistical significance, a
450 consistent tendency to lower pAkt/Akt ratio was detectable at 24h (Fig. 6D) as well as
451 detectably higher FOXO3 levels in both the nuclei and the cytosol at 12h of treatment
452 (Supplementary Figure 3). All together these results suggest that FOXO3 activity is more
453 likely to play a relevant role in antioxidant gene regulation in galactose than in glucose
454 cultured cells.

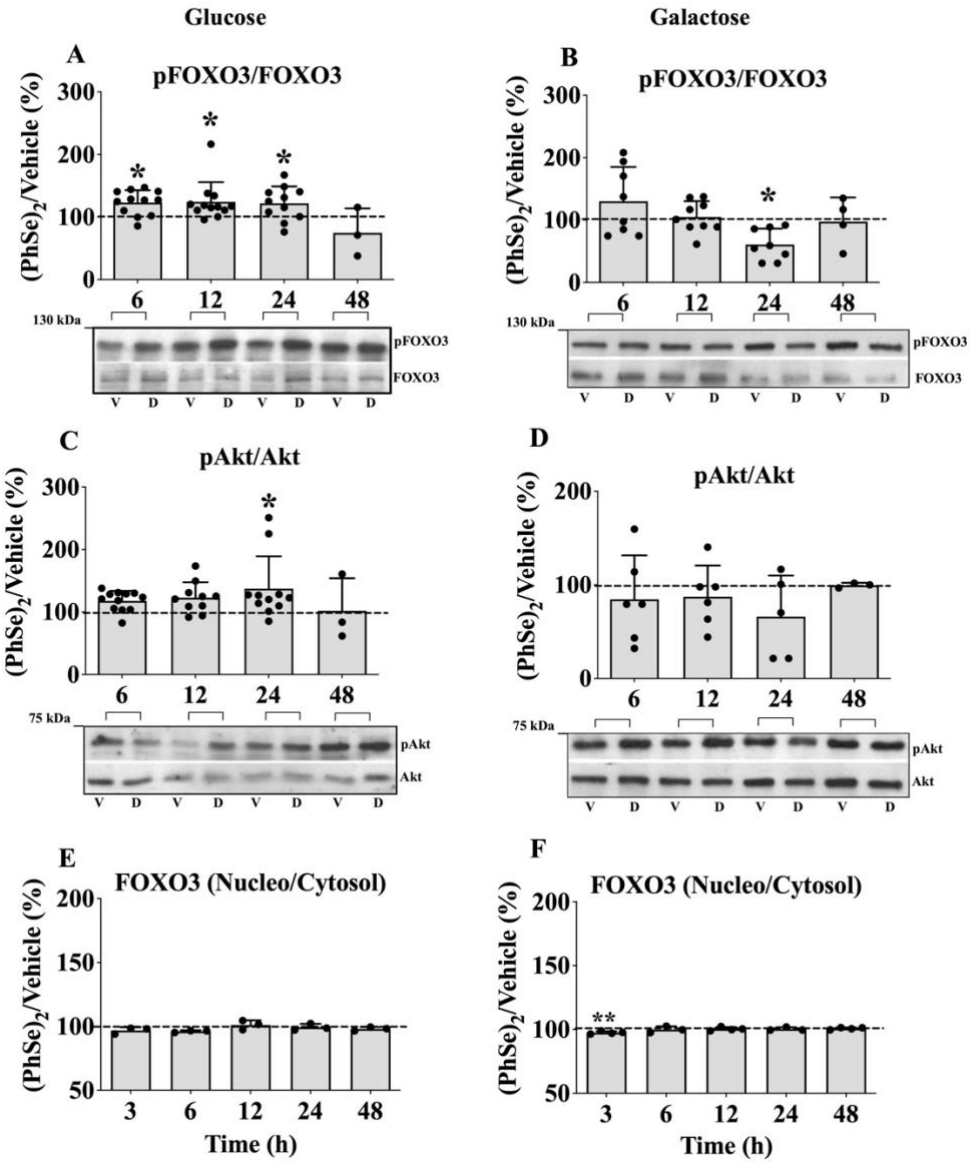

Fig. 6 Effect of $(PhSe)_2$ on pFOXO3 and pAkt levels in BAEC conditioned in glucose- or galactose-containing medium. BAEC were treated with $(PhSe)_2$ or vehicle (DMSO) for 3, 6, 12, 24 and 48h in glucose (A, C and E) or galactose (B, D and F) medium to analyze pFOXO3 (A-B) and pAkt (C-D) protein content by Western blotting. Results are expressed as protein/β-tubulin or FOXO3 ratio and the data is presented as the relative % of treatment with $(PhSe)_2$ (bars) *vs* vehicle. V = vehicle, D = $(PhSe)_2$. (E and F) Immunofluorescence for FOXO3 were analyzed. Ratio of FOXO3 in the nuclei/cytosol. Data were represented as mean ± SD (n=3-13). * $p < 0.05$, indicate statistical difference from vehicle group (dashed line) by two-way ANOVA, followed by Bonferroni's *post hoc* test.

4. Discussion

468 Endothelial cells are the primary target of circulating redox-active molecules.
469 Among these, primary bovine aortic endothelial cells (BAEC), since preserving their
470 original metabolic plasticity, represent a relevant *in vitro* model for investigating the
471 effects of pharmacological agents across diverse metabolic contexts. The choice of cell
472 culture media profoundly influences the metabolic performance of cells *in vitro.* Our
473 recent findings, particularly concerning the modulation of transcription factors Nrf2 and
474 FOXO3 key regulators of antioxidant gene expression in BAECs, underscore the
475 significance of cellular metabolic state. Specifically, alterations in cell culture conditions,
476 leading to heightened reliance on oxidative metabolism, demonstrate a consequential
477 impact on the efficacy of redox-active agents on vascular cells. These observations
478 suggest that the effectiveness of redox-active agents on endothelial cells may be
479 intricately linked to their metabolic milieu. Therefore, we investigate the effects of
480 $(PhSe)_2$ on BAEC cultured in media containing glucose or galactose, assessing its impact
481 on metabolism and antioxidant responses.

482 $(PhSe)_2$ has been extensively studied for its pivotal role in vascular physiology
483 and pathology, attributed to its capacity for redox modulation. This includes the
484 promotion of mitochondrial respiration and the upregulation of antioxidant gene
485 expression, partly mediated by the translocation of Nrf2 to the nucleus [22]. Our findings
486 reveal significant differences in the action of $(PhSe)_2$ depending on whether BAEC are
487 cultured in galactose and glucose media. These differences are likely to be relevant to
488 their vascular effects *in vivo*. In cells cultured in glucose, treatment with $(PhSe)_2$ yielded
489 a net positive impact on mitochondrial oxidative capacity, assessed by respirometry. This
490 enhancement correlated with observed changes in mitochondrial cellular dynamics,
491 characterized by more fused mitochondria and a uniform distribution of mitochondria
492 throughout the cells, with reduced concentration in the perinuclear region. Conversely,

493 these changes were not observed in cells cultured with galactose, where the cells were
494 already compelled to utilize their oxidative capacity. Therefore, the modulation of
495 mitochondrial function by $(PhSe)_2$ appears to be effective only in cells exhibiting limited
496 utilization of their mitochondrial oxidative capacity. Regarding $(PhSe)_2$ antioxidant
497 capacity, we noted that although $(PhSe)_2$ induces the nuclear translocation of Nrf2 in both
498 glucose and galactose media, Nrf2 remains longer in the nuclei of cells cultured in
499 galactose media. This observation suggests a potential preference for nuclear retention in
500 the galactose environment. However, any speculation regarding the underlying
501 mechanism at this stage would be highly conjectural. Potential explanations could involve
502 interactions with other transcription factors [29] or the inhibition of its nuclear extrusion
503 [30].

504 The enhanced Nrf2 activation profile observed in galactose media is even more
505 pronounced in the case of FOXO3a, where its activation is solely detectable in galactose
506 media, with reduced levels of pFOXO3a and increased nuclear protein levels. This shared
507 pattern suggests a more efficient induction of antioxidant gene expression in galactose
508 compared to glucose media. However, analysis of the gene expression changes elicited
509 by $(PhSe)_2$ on crucial antioxidant genes controlling mitochondrial antioxidant capacity
510 and glutathione synthesis and recycling reveals a stronger induction in glucose media. In
511 galactose media, the changes induced by $(PhSe)_2$ are not only smaller but also
512 predominantly focused on glutathione homeostasis, suggesting a more cytosolic, rather
513 than mitochondrial effect. Therefore, the induction of antioxidants genes by $(PhSe)_2$ in
514 glucose media likely requires additional transcription factors that are especially active in
515 conditions of low mitochondrial activity. Potential candidates include NFkB [31] a redox-
516 sensitive transcription factor controlling antioxidant gene expression, and c-MYC [32]
517 among others. Additionally, since $(PhSe)_2$ also enhances mitochondrial fission and

518 maximal oxidative capacity, other pathways may be involved. Acute inhibition of
519 mitochondrial respiration could drive compensatory mechanisms, such as the activation
520 of PGC-1α, which can induce both antioxidant gene expression and mitochondrial fusion
521 [8] while supporting FOXO3 [13] and Nrf2 [14] activation.

522 Despite the apparent lower capacity of $(PhSe)_2$ to induce antioxidant gene
523 expression in galactose media, assessments of mitochondrial antioxidant capacity using
524 the mitochondrial inhibitor DMNQ or the exogenous addition of H_2O_2 suggest a
525 potentially heightened antioxidant response in galactose-treated cells. This inference
526 arises from the substantial reduction elicited by $(PhSe)_2$ on mitochondrial superoxide (O_2^-
527) levels in galactose-cultured cells following a challenge with H_2O_2. However, drawing
528 definitive conclusions from these observations is challenging. In galactose media, cells
529 exhibit greater resistance to DMNQ, while in glucose media, they are highly susceptible
530 to H_2O_2-induced mitochondrial damage, resulting in under basal levels of mitochondrial
531 O_2^-. Notably, $(PhSe)_2$ partially rescues these aberrant levels and restores them to normal,
532 consistent with its observed capacity to enhance mitochondrial oxidative capacity.

533 Therefore, our data suggest that while $(PhSe)_2$ demonstrates greater efficacy in the
534 activation of Nrf2 and FOXO3a under pro-oxidative conditions, alternative pathways
535 contribute to its enhancement of mitochondrial oxidative capacity and total antioxidant
536 capacity when cells are cultured in glucose media. The observation that $(PhSe)_2$ induces
537 acute inhibition of mitochondrial respiration shortly after treatment may indicate a
538 significant role for mitochondrial function in this context. In summary, our findings
539 underscore the critical influence of the cellular metabolic status on antioxidant capacity
540 of redox-active molecules such as $(PhSe)_2$.

541 **Declaration of competing interest**

The authors declare that they have no known competing financial interests or personal relationships that could have appeared to influence the work reported in this paper.

Acknowledgments

This work was supported by MCIN/AEI/10.13039/501100011033/FEDER, UE, [grant numbers RTI2018-093864-B-I00 and PID2021-122765OB-I00]; the European Union's Horizon 2020 research and innovation programme under the Marie Skłodowska-Curie [grant agreement 721236-TREATMENT]; EU Horizon Europe Program under the EIC Pathfinder DiBaN [GA-101162517]; the Brazilian institutions: Conselho Nacional de Desenvolvimento Científico e Tecnológico (CNPq), Coordenação de Aperfeiçoamento de Pessoal de Nível Superior (CAPES), Fundação de Apoio à Pesquisa do Distrito Federal (FAPDF) [grants 00193-00000884/2021-89 and 00193-00002348/2022-07]; and Instituto Nacional de Ciência e Tecnologia e Neuro-ImunoModulação (INCT-NIM) [grant 485489/2014-1]. The authors are grateful to Smart Servier Biology Medicine for the available figures.

References

[1] Z. Abbaszadeh, S. Çeşmeli, Ç. Biray Avcı, Crucial players in glycolysis: Cancer progress, Gene, 726 (2020).

[2] Y. Liu, K. Birsoy, Metabolic sensing and control in mitochondria, Mol Cell, 83 (2023) 877–889.

[3] E.A. Zaal, C.R. Berkers, The influence of metabolism on drug response in cancer, Front Oncol, 8 (2018).

[4] M.J.C. de Kok, A.F. Schaapherder, R.C.I. Wüst, M. Zuiderwijk, J.A. Bakker, J.H.N. Lindeman, S.E. Le Dévédec, Circumventing the Crabtree effect in cell culture: A systematic review, Mitochondrion, 59 (2021) 83–95.

[5] L.D. Marroquin, J. Hynes, J.A. Dykens, J.D. Jamieson, Y. Will, Circumventing the crabtree effect: Replacing media glucose with galactose increases susceptibility of hepG2 cells to mitochondrial toxicants, Toxicological Sciences, 97 (2007) 539–547.

[6] V.M. Gohil, S.A. Sheth, R. Nilsson, A.P. Wojtovich, J.H. Lee, F. Perocchi, W. Chen, C.B. Clish, C. Ayata, P.S. Brookes, V.K. Mootha, Nutrient-sensitized screening for drugs that shift energy metabolism from mitochondrial respiration to glycolysis, Nat Biotechnol, 28 (2010) 249–255.

575 [7] M. V. Golikov, V.T. Valuev-Elliston, O.A. Smirnova, A. V. Ivanov,
576 Physiological Media in Studies of Cell Metabolism, Mol Biol, 56 (2022) 629–
577 637.
578 [8] I. Valle, A. Álvarez-Barrientos, E. Arza, S. Lamas, M. Monsalve, PGC-1α
579 regulates the mitochondrial antioxidant defense system in vascular endothelial
580 cells, Cardiovasc Res, 66 (2005) 562–573.
581 [9] V. Ngo, M.L. Duennwald, Nrf2 and Oxidative Stress: A General Overview of
582 Mechanisms and Implications in Human Disease, Antioxidants, 11 (2022).
583 [10] K.A. Lasick, E. Jose, A.M. Samayoa, L. Shanks, K.W. Pond, C.A. Thorne, A.L.
584 Paek, FOXO nuclear shuttling dynamics are stimulus-dependent and correspond
585 with cell fate, Mol Biol Cell, 34 (2023).
586 [11] J.M. Deblasi, G.M. Denicola, Dissecting the crosstalk between nrf2 signaling and
587 metabolic processes in cancer, Cancers (Basel), 12 (2020) 1–20.
588 [12] M. Monsalve, Y. Olmos, The Complex Biology of FOXO, 2011.
589 [13] I. Valle, Y. Olmos, S. Borniquel, A. Tierrez, E. Soria, S. Lamas, M. Monsalve,
590 Mutual dependence of Foxo3a and PGC-1α in the induction of Oxidative stress
591 genes, Journal of Biological Chemistry, 284 (2005) 14476–14484.
592 [14] E. Navarro, L. Gonzalez-Lafuente, I. Pérez-Liébana, I. Buendia, E. López-
593 Bernardo, C. Sánchez-Ramos, I. Prieto, A. Cuadrado, J. Satrustegui, S. Cadenas,
594 M. Monsalve, M.G. López, Heme-Oxygenase i and PCG-1α Regulate
595 Mitochondrial Biogenesis via Microglial Activation of Alpha7 Nicotinic
596 Acetylcholine Receptors Using PNU282987, Antioxid Redox Signal, 27 (2017)
597 93–105.
598 [15] L.S. Galant, L. Doblado, R. Radi, A.F. de Bem, M. Monsalve, Culture of Bovine
599 Aortic Endothelial Cells in Galactose Media Enhances Mitochondrial Plasticity
600 and Changes Redox Sensing, Altering Nrf2 and FOXO3 Levels, Antioxidants, 13
601 (2024).
602 [16] B. Fiuza, N. Subelzú, P. Calcerrada, M.R. Straliotto, L. Piacenza, A. Cassina,
603 J.B.T. Rocha, R. Radi, A.F. De Bem, G. Peluffo, Impact of SIN-1-derived
604 peroxynitrite flux on endothelial cell redox homeostasis and bioenergetics:
605 Protective role of diphenyl diselenide via induction of peroxiredoxins, Free Radic
606 Res, 49 (2015) 122–132.
607 [17] A.F. De Bem, B. Fiuza, P. Calcerrada, P.M. Brito, G. Peluffo, T.C.P. Dinis, M.
608 Trujillo, J.B.T. Rocha, R. Radi, L.M. Almeida, Protective effect of diphenyl
609 diselenide against peroxynitrite-mediated endothelial cell death: A comparison
610 with ebselen, Nitric Oxide, 31 (2013) 20–30.
611 [18] M.A. Hort, M.R. Straliotto, P.M. Netto, J. Batista Teixeira Da Rocha, A. Fabro
612 De Bem, R.M. Ribeiro-Do-Valle, Diphenyl Diselenide Effectively Reduces
613 Atherosclerotic Lesions in LDLr 2/2 Mice by Attenuation of Oxidative Stress and
614 Inflammation, n.d.
615 [19] M.R. Straliotto, M.A. Hort, B. Fiuza, J.B.T. Rocha, M. Farina, G. Chiabrando,
616 A.F. De Bem, Diphenyl diselenide modulates oxLDL-induced cytotoxicity in
617 macrophage by improving the redox signaling, Biochimie, 95 (2013) 1544–1551.
618 [20] A.F. de Bem, M. Farina, R. de L. Portella, C.W. Nogueira, T.C.P. Dinis, J.A.N.
619 Laranjinha, L.M. Almeida, J.B.T. Rocha, Diphenyl diselenide, a simple
620 glutathione peroxidase mimetic, inhibits human LDL oxidation in vitro,
621 Atherosclerosis, 201 (2008) 92–100.
622 [21] S.G. Müller, N.S. Jardim, C.B. Quines, C.W. Nogueira, Diphenyl diselenide
623 regulates Nrf2/Keap-1 signaling pathway and counteracts hepatic oxidative stress
624 induced by bisphenol A in male mice, Environ Res, 164 (2018) 280–287.

[22] R.L. Quispe, M.L. Jaramillo, L.S. Galant, D. Engel, A.L. Dafre, J.B. Teixeira da Rocha, R. Radi, M. Farina, A.F. de Bem, Diphenyl diselenide protects neuronal cells against oxidative stress and mitochondrial dysfunction: Involvement of the glutathione-dependent antioxidant system, Redox Biol, 20 (2019) 118–129.

[23] D. Bartolini, J. Commodi, M. Piroddi, L. Incipini, L. Sancineto, C. Santi, F. Galli, Glutathione S-transferase pi expression regulates the Nrf2-dependent response to hormetic diselenides, Free Radic Biol Med, 88 (2015) 466–480.

[24] M. Monsalve, S. Borniquel, I. Valle, S. Lamas, Mitochondrial dysfunction in human pathologies, 2007.

[25] G. Peluffo, P. Calcerrada, L. Piacenza, N. Pizzano, R. Radi, Superoxide-mediated inactivation of nitric oxide and peroxynitrite formation by tobacco smoke in vascular endothelium: studies in cultured cells and smokers, Am J Physiol Heart Circ Physiol, 296 (2009) 1781–1792.

[26] S. Borniquel, N. García-Quintáns, I. Valle, Y. Olmos, B. Wild, F. Martínez-Granero, E. Soria, S. Lamas, M. Monsalve, Inactivation of Foxo3a and Subsequent Downregulation of PGC-1α Mediate Nitric Oxide-Induced Endothelial Cell Migration, Mol Cell Biol, 30 (2010) 4035–4044.

[27] J. Bernal-Tirapo, M.T. Bayo Jiménez, P. Yuste-García, I. Cordova, A. Peñas, F.J. García-Borda, C. Quintela, I. Prieto, C. Sánchez-Ramos, E. Ferrero-Herrero, M. Monsalve, Evaluation of Mitochondrial Function in Blood Samples Shows Distinct Patterns in Subjects with Thyroid Carcinoma from Those with Hyperplasia, Int J Mol Sci, 24 (2023).

[28] F. He, X. Ru, T. Wen, NRF2, a transcription factor for stress response and beyond, Int J Mol Sci, 21 (2020) 1–23.

[29] W. Li, S. Yu, T. Liu, J.H. Kim, V. Blank, H. Li, A.N.T. Kong, Heterodimerization with small Maf proteins enhances nuclear retention of Nrf2 via masking the NESzip motif, Biochim Biophys Acta Mol Cell Res, 1783 (2008) 1847–1856.

[30] J.W. Kaspar, A.K. Jaiswal, Tyrosine phosphorylation controls nuclear export of Fyn, allowing Nrf2 activation of cytoprotective gene expression, The FASEB Journal, 25 (2011) 1076–1087.

[31] M.J. Morgan, Z.G. Liu, Crosstalk of reactive oxygen species and NF-κB signaling, Cell Res, 21 (2011) 103–115.

[32] D.R. Wonsey, K.I. Zeller, C. V Dang, The c-Myc target gene PRDX3 is required for mitochondrial homeostasis and neoplastic transformation, n.d.